NUCLEAR SCIENCE AND ENGINEERING: **169**, 178–187 (2011)

Gas Production in the MEGAPIE Spallation Target

Nicolas Thiollière,[a]* Luca Zanini,[b] Jean-Christophe David,[c] Jost Eikenberg,[b] Arnaud Guertin,[a]
Alexander Yu. Konobeyev,[d] Sébastien Lemaire,[e] and Stefano Panebianco[c]

[a]*SUBATECH, EMN-IN2P3/CNRS-Université, Nantes F-44307, France*
[b]*Paul Scherrer Institut, 5232 Villigen PSI, Switzerland*
[c]*CEA Saclay, Irfu/SPhN, 91191 Gif Sur Yvette, France*
[d]*Institut für Reaktorsicherheit, FZK GmbH, 76021 Karlsruhe, Germany*
[e]*CEA Bruyères-le-Châtel, DAM Ile de France, 91297 Arpajon cedex, France*

Received July 1, 2010
Accepted February 28, 2011

Abstract—*The MEGAwatt PIlot Experiment (MEGAPIE) project was started in 2000 to design, build, and operate a liquid lead-bismuth eutectic (LBE) spallation neutron target at the power level of 1 MW. The target was irradiated for 4 months in 2006 at the Paul Scherrer Institute in Switzerland. Gas samples were extracted in various phases of operation and analyzed by γ spectroscopy, leading to the determination of the main radioactive isotopes released from the LBE. Comparison with calculations performed using several validated codes (MCNPX2.5.0/CINDER'90, FLUKA/ORIHET, and SNT) yields the ratio between simulated in-target isotope production rates and experimental amounts released at any given time. This work underlines the weak points of spallation models for some released isotopes. Also, results provide relevant information for safety and radioprotection in an accelerator-driven system and more particularly for the gas management in a spallation target dedicated to neutron production facilities.*

I. INTRODUCTION

The feasibility of an accelerator driven-system[1] (ADS) to transmute minor actinides is one of the major issues related to nuclear waste management. An ADS is composed of three elementary components widely studied separately in dedicated programs and experiments: the high-energy proton beam, the spallation target, and the subcritical core.

The MEGAwatt PIlot Experiment (MEGAPIE) project[2] was started in 2000 to design, build, operate, and dismantle a 1-MW liquid lead-bismuth eutectic (LBE) spallation target irradiated by a 575-MeV proton beam. The MEGAPIE target was installed at the Swiss Spallation Neutron Source SINQ at the Paul Scherrer Institute (PSI) in Villigen, Switzerland, at the end of 2005 and was irradiated from August to December 2006. Figure 1 shows a schematic view of the MEGAPIE target underlining the main components: the liquid lead-bismuth target; the structural materials, such as the beam window (T91 steel) and the LBE container (316L steel); the central rod containing neutron detectors; and the expansion volume, which collects the released gases. Table I provides the main parameters of the MEGAPIE target.

Nuclear and neutronic assessment of the target has been performed during the project.[3] The main goal of this paper is to provide relevant information on the gas production problematic in a spallation target, which is identified as one of the main drawbacks of ADS with respect to fast reactor systems as nuclear waste incinerators.[4] Indeed, hydrogen and helium production causes embrittlement by swelling on structural materials. In addition, the high amount of radioactive volatile isotopes that ends in the gas-handling system, called the cover gas system (CGS), requires specific safety measures during handling operations or in case of an accident. In particular, the possible release of polonium isotopes (208, 209, and 210 isotopes) would induce a high α activity and hence a serious safety issue.

After their production inside the target, volatile isotopes diffuse within the LBE and a fraction of them can be released at the level of the liquid metal free surface. These processes are very complex.[5] As the LBE circulates in a closed loop, both diffusion and convection contribute to isotopic displacement inside the target. Some chemical recombinations are possible, such as

*E-mail: nicolas.thiolliere@subatech.in2p3.fr

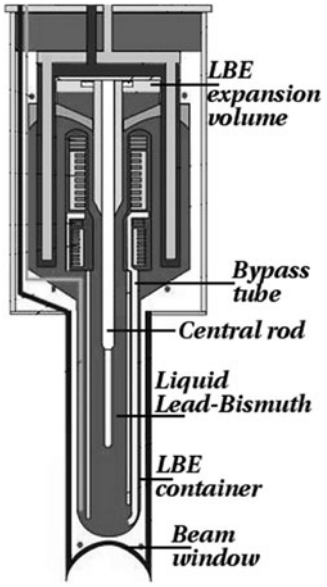

Fig. 1. MEGAPIE target schematic view.

TABLE I

Main Parameters of the MEGAPIE Target

Main specifications	
Length	5.35 m
Diameter lower part	10.6 cm
LBE volume	~82 ℓ
Beam parameters	
Proton beam energy	575 MeV
Maximum intensity	1.35 mA
Operation parameters	
LBE temperature range	240°C to 380°C
Maximum LBE flow velocity	1.2 m/s
Window temperature range	330°C to 380°C

oxide formation with the oxygen generated by spallation reactions, chemical reactions with structural materials, or deposition at cold surfaces. It is possible to classify volatile isotopes into specific groups according to the specific reaction by which they are produced from the interaction between the proton beam and the LBE:

1. H and He produced by intranuclear cascade and evaporation
2. Kr, Xe, and I, produced by fission
3. Ne, created by both evaporation and fission
4. Hg, produced by the intranuclear cascade process
5. Po, generated by (p, xn) reactions on Bi, (α, xn) reactions on Pb, (n, γ) on ^{209}Bi and subsequent beta decay to ^{210}Po, or α or π exchange reactions on Bi leading to At and subsequent decay to Po.

During the MEGAPIE experiment gas measurements were performed in order to assess as many as possible of these produced isotopes.

II. GAS AND VOLATILE MEASUREMENTS

The CGS was connected to an expansion volume located at the top of the target where the released isotopes were collected. Figure 2 shows a schematic view of the CGS, including the target expansion volume, the decay tank for the storage of radioactive gas, the sampling unit dedicated to activity measurement, and some pressure transducers.

Two fresh gas samplings were performed 2 days after the beginning of operation, which corresponds to 1 mA·h of accumulated charge on target. The first gas-sampling procedure consisted of venting the expansion volume into the sampling unit. This was followed by a dilution in the decay tank and the sampling unit was then removed to be analyzed. The second fresh gas sampling was performed by venting a low fraction of the gas contained in the decay tank into a second sampling unit. The two sampling units were analyzed by gamma spectroscopy (see Fig. 3 for a typical gamma spectrum from the first gas sample). The activities with their uncertainties obtained from the analysis of the two samples are presented in Table II. Noble gases such as argon, krypton, and xenon were detected. Heavier nuclide activities were also measured and underline the presence of gold and mercury. Note that detected gold isotopes are due to mercury decay. We notice the following two important points:

1. Neither mercury nor gold was detected in the second sample.

2. Noble gas activities were approximately 40% lower in comparison with the first sample, and this deviation does not depend on isotope mass.

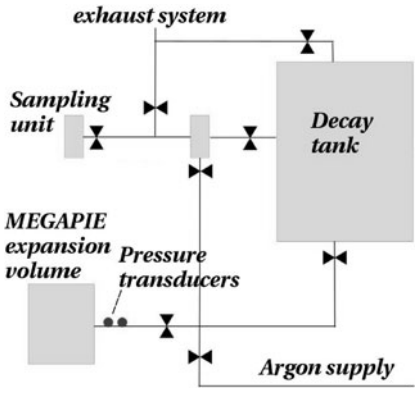

Fig. 2. Schematic view of the CGS.

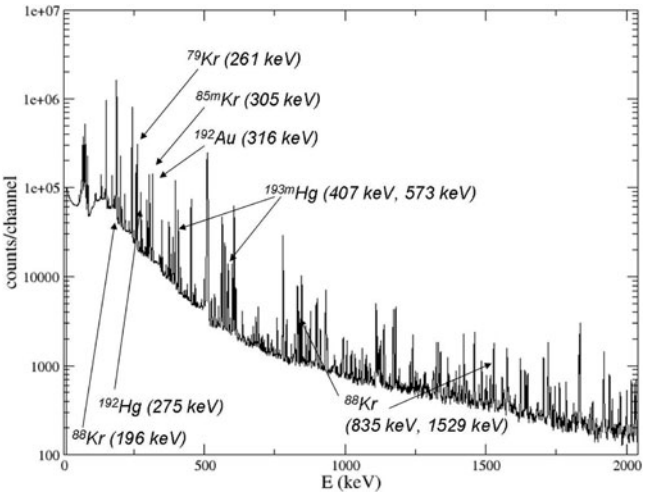

Fig. 3. First fresh gas sample gamma spectrum with relevant γ lines.

TABLE II

Isotopes' Half-Lives and Measured Activities, with Associated Uncertainty in the First Gas Sample

Nuclide	$T_{1/2}$	Activity (Bq)	
		Sample 1	Sample 2
^{41}Ar	1.8 h	3.2×10^2 (20%)	2.4×10^2 (20%)
^{79}Kr	34.9 h	4.5×10^4 (5%)	3.1×10^4 (5%)
^{85m}Kr	4.5 h	1.5×10^5 (5%)	1.1×10^5 (5%)
^{88}Kr	2.8 h	2.7×10^4 (5%)	1.9×10^4 (5%)
^{122}Xe	20.1 h	1.4×10^4 (10%)	9.3×10^3 (5%)
^{125}Xe	16.9 h	9.5×10^4 (5%)	6.5×10^4 (5%)
^{127}Xe	36.4 days	5.0×10^3 (5%)	3.6×10^3 (5%)
^{129m}Xe	8.9 days	7.6×10^3 (5%)	3.9×10^3 (50%)
^{135}Xe	9.1 h	5.7×10^2 (10%)	3.6×10^2 (5%)
^{192}Au	5.0 h	3.4×10^4 (5%)	—
^{193}Au	17.7 h	1.2×10^4 (10%)	—
^{195}Au	186 days	1.2×10^2 (15%)	—
^{192}Hg	4.9 h	1.8×10^4 (5%)	—
^{193m}Hg	11.8 h	1.2×10^4 (5%)	—
^{195m}Hg	41.6 h	2.9×10^3 (5%)	—
^{197}Hg	64.1 h	2.1×10^4 (5%)	—
^{197m}Hg	23.8 h	3.6×10^3 (5%)	—
^{203}Hg	46.6 days	5.0×10^1 (5%)	—

The latter result gives an order of magnitude on the systematic uncertainty in the noble gas measurements since according to the sampling procedure, the amount of radioactive gases in both samples should have been the same. The behavior of the mercury isotopes is more difficult to interpret, but it seems to indicate that a fraction of the heavier isotopes have stuck to the pipe walls or the decay tank during the second sampling operation.

To correlate experimental activities presented in Table II with the activity in the expansion volume, which contains information on the actual volatile elements released, we define two groups, the noble gases and mercury, showing a similar behavior from the production to the detection of their isotopes. Indeed, Ar, Kr, and Xe are chemically inert noble gases with high volatility. It is thus reasonable to consider that noble gas behavior will be ruled by similar mechanisms.[5] The noble gases are considered as fully volatile during the sampling procedure. The gold isotopes are assumed to come from decay of mercury effused from the expansion volume to the sampling unit. The absence of Hg and Au in the second sample could be due to three possible scenarios that cover all possibilities that could occur in the CGS:

Scenario s1: Mercury and gold are fully volatile during all the steps of the procedure. This is the standard scenario that is considered for the measured noble gases. However, this scenario is only theoretical because Hg and Au were observed only in the first sample.

Scenario s2: All the mercury and gold diffuse into the first sampling unit and an unknown proportion sticks on the sampling unit, the decay tank walls, and the linking pipes.

Scenario s3: Mercury and gold stick on the pipes and walls somewhere between the expansion volume and the sampling unit even before the first sampling.

Each scenario has a specific normalization factor, called sampling factor S, to be applied on the measured activity $A_{e\text{-}S}$ in order to obtain the activity in the MEGAPIE expansion volume $A_{e\text{-}EV}$. This factor is defined as

$$A_{e\text{-}EV} = S \times A_{e\text{-}S} \ . \qquad (1)$$

The sampling factor represents the ratio between the number of atoms in the expansion volume and that in the sampling unit (see Fig. 2). This ratio can be calculated by equating the pressure in the expansion volume to that in the rest of the system. Perfect gas behavior is also assumed and volumes and temperatures are known with sufficient accuracy. Note that the temperature in the expansion volume is different from the temperature in the rest of the CGS.

For scenario s1, we have calculated a sampling factor $S_{s1} = 3.33 \times 10^3$. This value is also used for the estimation of noble gas activity in the expansion volume.

For scenario s2, the sampling factor value depends on the gas proportion that has stuck on the sampling unit walls. Therefore, it is contained within two limits. The lower limit represents the case where all the mercury has stuck before the dilution into the decay tank while the upper limit is the case described by scenario s1. The calculation gives a scenario s2 with a sampling factor $25 \leq S_{s2} \leq 3.33 \times 10^3$.

The lower limit of the third scenario corresponds to the mercury normal diffusion up to the sampling unit (represented then by scenario s2). A calculation where all the mercury is sticking on the pipes between the expansion volume and the sampling unit gives the upper limit of scenario s3, which leads to an infinite value of the sampling factor. The third scenario is then illustrated by the relation $25 \leq S_{s3} \leq \infty$.

Since there is no argument for choosing between scenarios s2 and s3, the sampling factor can be defined only by its lower limit:

$$S \geq 25 \quad . \tag{2}$$

III. GAS AND VOLATILE PRODUCTION CALCULATIONS

In this section we compare the experimental activities with a set of calculations. We have employed several combinations of validated multiparticle transport codes coupled with evolution codes; in particular, FLUKA (Ref. 6) and MCNPX2.5.0 (Ref. 7)/CINDER'90 (Ref. 8). In addition, we have made calculations using the SNT code.[9] Concerning the MCNPX code, the most realistic set of spallation models describing the intranuclear cascade and the evaporation process have been defined after a detailed benchmark.[10,11] As a consequence, we carried out calculations with Bertini[12]/Dresner,[13] INCL4 (Ref. 14)/ABLA (Ref. 15), ISABEL (Ref.16)/ABLA (Ref. 15), and CEM2k (Ref. 17). A neutronic study has shown an agreement between simulated and experimental neutron flux[18] outside the target, thus validating the simulated geometry used. The evolution calculation takes into account the experimental irradiation time profile, which includes 15 h of cooling before the sample activity measurement (see Fig. 4). For each isotope excluding gold, the evolution takes into account spallation reactions, and decay and nuclear reactions with low-energy neutrons (i.e., $E < 20$ MeV). Gold is not volatile and it is assumed to be generated only from the decay of released mercury. Its spallation production rate is then initialized to zero in the evolution calculation.

Table II shows that we could measure some metastable nuclide activities. The metastable production with MCNPX is taken into account via a data library used in the gamma emission module.[19] With FLUKA, the isomeric production ratio is 0.5 for all nuclides. The yields of nuclei in metastable states induced by neutrons are simulated in SNT from the evaluations available in the European Activation File[20] at energies <20 MeV. For higher energies the isomeric ratio is taken to be 0.5 for all cases. For proton-induced reactions the code SNT uses the Proton Activation Data File[21] below 150 MeV including accurate evaluations for isomer yields. Above 150 MeV, the ratio is 0.5 once more.

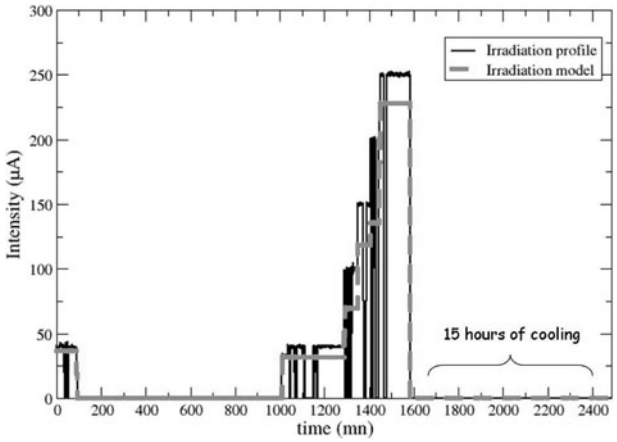

Fig. 4. Irradiation at the start-up of MEGAPIE. The dashed lines represent the irradiation model used in evolution calculations.

Results from the calculations are given in Table III. Statistical uncertainties on provided activities are not directly computable since after the evolution calculation, they are a combination of the nuclide production uncertainties, the nuclide's parents production uncertainties, and the neutron flux. We mention in the table the uncertainty on independent spallation rate production provided by simulation codes when available. This represents an underestimation of the statistical error, but it remains an acceptable order of magnitude.

Simulation codes provide the evaluation of isotope production inside the LBE while measurements give the production released from the target. Moreover, a release fraction is defined as the amount of released atoms per produced atom in the LBE at the time of the measurement. The ratio between released and simulated in-target isotope values could be interpreted as the evaluation of the release fraction for the spallation model used at the time the measurement is made.

IV. GAS AND VOLATILE RELEASE PARAMETER ESTIMATION

For each code and model combination and for each measured isotope, the ratio $R(t_{irr})$ between experimental activity in the expansion volume and simulated in-target production has been extracted as

$$R(t_{irr}) = \frac{A_{e\text{-}EV}}{A_{s\text{-}IT}} = S \times \frac{A_{e\text{-}S}}{A_{s\text{-}IT}} \quad . \tag{3}$$

This number depends on the irradiation profile and on the time the measurement is made, which we summarize by the variable t_{irr}. S is the sampling factor defined above. $A_{e\text{-}EV}$, $A_{e\text{-}S}$, and $A_{s\text{-}IT}$ are the experimental activity

TABLE III

Activities Measured (Probe 1) and Calculated with Different Model Combinations of MCNPX and with FLUKA and SNT*

Nuclide	Probe 1	MCNPX				FLUKA 2008	SNT
		Bertini/Dresner	INCL4/ABLA	ISABEL/ABLA	CEM		
^{41}Ar	3.2×10^2 (20)[a]	3.6×10^4 (10)	1.4×10^4 (10)	2.1×10^4 (10)	1.5×10^3 (25)	1.1×10^4	2.7×10^2
^{79}Kr	4.5×10^4 (5)	5.2×10^6 (3)	2.4×10^6 (4)	3.1×10^6 (3)	7.3×10^6 (2)	2.8×10^6	5.2×10^6
^{85m}Kr	1.5×10^5 (5)	1.1×10^7 (2)	1.5×10^7 (1)	1.2×10^7 (1)	1.0×10^7 (1)	2.0×10^7	5.3×10^6
^{88}Kr	2.7×10^4 (5)	2.7×10^6 (2)	2.0×10^6 (2)	1.4×10^6 (3)	8.5×10^5 (2)	2.2×10^6	1.3×10^6
^{122}Xe	1.4×10^4 (10)	2.7×10^6 (4)	1.2×10^6 (7)	1.6×10^6 (6)	1.1×10^6 (5)	6.6×10^5	2.6×10^6
^{125}Xe	9.5×10^4 (5)	6.2×10^6 (4)	5.1×10^6 (4)	5.6×10^6 (4)	3.9×10^6 (3)	3.8×10^6	8.2×10^6
^{127}Xe	5.0×10^3 (5)	3.4×10^5 (3)	2.7×10^5 (4)	3.1×10^5 (4)	2.2×10^5 (3)	2.8×10^5	4.0×10^5
^{129m}Xe	7.6×10^3 (5)	1.2×10^5 (3)	9.2×10^4 (4)	1.4×10^5 (4)	6.0×10^4 (3)	2.7×10^5	1.2×10^{-2}
^{135}Xe	5.7×10^2 (10)	2.3×10^6 (6)	1.4×10^5 (19)	9.9×10^4 (29)	6.5×10^4 (22)	1.3×10^5	7.2×10^4
^{192}Au	3.4×10^4 (5)	8.4×10^8 (0)	9.6×10^8 (0)	1.0×10^9 (0)	1.3×10^9 (0)	1.0×10^9	1.4×10^9
^{193}Au	1.2×10^4 (10)	8.0×10^8 (0)	8.7×10^8 (0)	9.1×10^8 (0)	1.0×10^9 (0)	9.5×10^8	1.2×10^9
^{195}Au	1.2×10^2 (15)	5.2×10^6 (0)	5.7×10^6 (0)	6.4×10^6 (0)	5.9×10^6 (0)	6.7×10^6	7.1×10^6
^{192}Hg	1.8×10^4 (5)	3.4×10^8 (0.3)	4.0×10^8 (0.5)	4.1×10^8 (0.5)	5.2×10^8 (0.3)	4.0×10^8	5.3×10^8
^{193m}Hg	1.2×10^4 (5)	1.7×10^8 (0.3)	1.3×10^8 (0.5)	1.3×10^8 (0.5)	1.1×10^8 (0.3)	8.7×10^7	5.0×10^7
^{195m}Hg	2.9×10^3 (5)	5.8×10^7 (0.4)	4.9×10^7 (0.5)	4.5×10^7 (0.5)	3.4×10^7 (0.4)	4.1×10^7	2.7×10^7
^{197}Hg	2.1×10^4 (5)	6.3×10^8 (0.5)	6.5×10^8 (0.5)	7.1×10^8 (0.6)	6.2×10^8 (0.4)	9.5×10^8	7.2×10^8
^{197m}Hg	3.6×10^3 (5)	6.6×10^7 (0.5)	6.7×10^7 (0.5)	5.3×10^7 (0.6)	4.4×10^7 (0.4)	4.2×10^7	5.7×10^7
^{203}Hg	5.0×10^1 (5)	2.2×10^6 (0.8)	2.5×10^6 (0.8)	1.8×10^6 (1)	9.9×10^5 (0.9)	7.8×10^5	1.4×10^6

*Activity values are expressed in Bq.

[a]Indicated uncertainty in parentheses (%) is the error on the isotope spallation production rate provided by the codes. Calculated values are obtained from the total activities in LBE divided by the sampling factor $S_{s1} = 3.33 \times 10^3$.

in the expansion volume and in the sampling unit and the simulated activity in the LBE target, respectively. Figure 5 shows the ratio $R(t_{irr})$ extracted for noble gases from the sampling factor S_{s1} as a function of mass number. The lower limit of the ratio $R(t_{irr})$ is also represented and estimated for gold and mercury from the sampling factor given by $S = 25$. We can distinguish two trends that discriminate noble gas and heavy nuclide behavior. Concerning the noble gases, the extracted ratio $R(t_{irr})$ is reasonably constant except for the case of ^{41}Ar calculated with the code SNT and ^{135}Xe calculated by Bertini/Dresner. For the first isotope, the model predicts a sharp decrease of

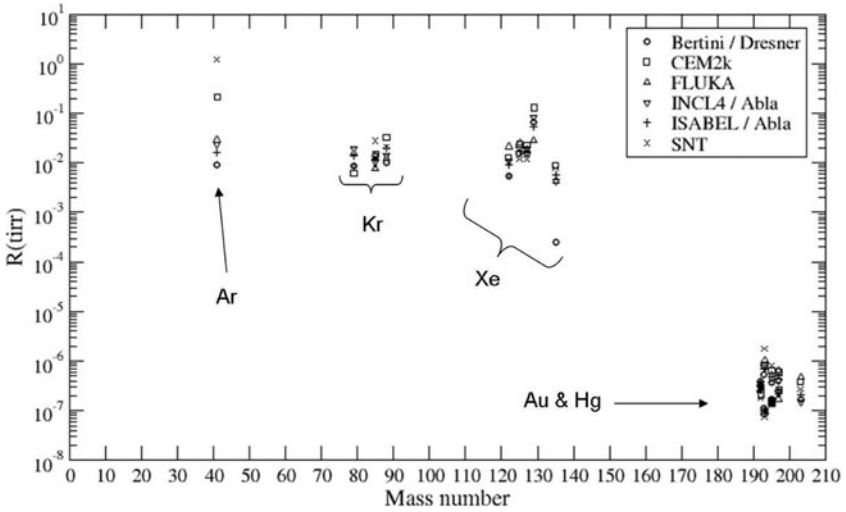

Fig. 5. $R(t_{irr})$ as a function of isotope mass number.

the fission yields for lead and bismuth isotopes with a decrease of the fragment mass for $A < 43$, which explains the strong deviation. The ^{135}Xe discrepancy is induced by the overestimated production rate using Bertini/Dresner. Argon-41 calculated with SNT and ^{135}Xe obtained with Bertini/Dresner are excluded for the calculation of the average value, and the error is extracted as the standard deviation coupled with the 40% of systematic error. The mean ratio $R(t_{irr})$ obtained for 1 mA·h of accumulated charge and 2 days of irradiation is given by

$$\langle R_{nb}(t_{irr})\rangle = (2.3 \pm 1.5)10^{-2} \quad . \tag{4}$$

Concerning heavy nuclides, we assume that the average ratio could be extracted as the mean value of the distribution while uncertainty is related to the distribution standard deviation and the 40% of systematic error. After 1 mA·h of accumulated charge and two days of operation, the lower limit of the ratio $R(t_{irr})$ is given by

$$\langle R_{\text{Hg-}s3}(t_{irr})\rangle = (3.4 \pm 2.9)10^{-7} \quad . \tag{5}$$

The ratio $R(t_{irr})$ for mercury shows the difficulty in understanding the mercury behavior in a complex system such as MEGAPIE.

To evaluate whether there is an effect of the nuclide half-life on the measurement results, we represented in Fig. 6 the ratio $R(t_{irr})$ as a function of isotope half-life. Figure 6 shows that there is no evident half-life effect in the calculated data for noble gases as well as for gold and mercury, as expected.

We calculate also the mass in the expansion volume obtained from the activity in the sampling unit multiplied by the sampling factor of scenario s1 in the case of noble gases. The lower limit of scenario s3 is used in the case of heavy nuclides, which means that the calculated lower limit on the produced mass in the expansion volume is given. Masses calculated by simulation are then multiplied by the noble gas ratio $R_{nb}(t_{irr})$ determined above [respectively the heavy nuclide ratio $R_{\text{Hg-}s3}(t_{irr})$]. Figures 7 and 8 show the mass distributions for xenon, gold, and mercury isotope production in the expansion volume of the MEGAPIE target.

To give a global view of the results, in Fig. 9 all points are represented as the ratio between experimental and simulated data. The dashed-dotted lines highlight a factor of 3 deviation from the experimental data, which shows the most important deviations and improvement necessities.

The following is devoted to the characterization of the release velocity from the LBE based on the most reliable calculations performed with INCL4/ABLA and CINDER'90 evolution codes. We define the probability $P_r(\Delta t)$ that a stable nuclide has to be released Δt after having been created[22]:

$$P_r(\Delta t) = 1 - \exp\left(-\frac{\Delta t}{\tau}\right) \quad . \tag{6}$$

The parameter τ represents the release velocity and depends on the LBE temperature. In our case, the release is weak so that Δt can be considered very small compared to τ. Thus,

$$P_r(\Delta t) \approx \frac{\Delta t}{\tau} \quad . \tag{7}$$

On the other hand, the probability $P_d(\Delta t)$ that a radioactive nuclide, with a radioactive constant λ, has not decayed Δt after its creation is given by

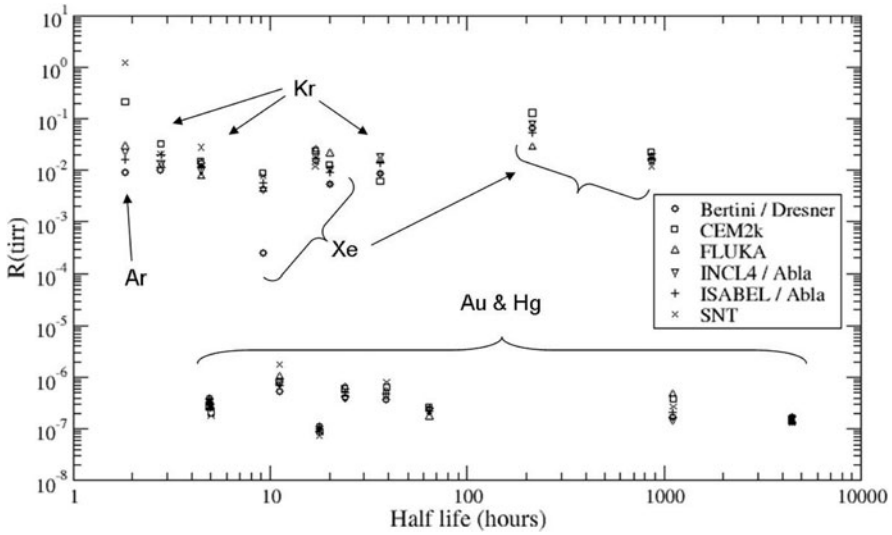

Fig. 6. $R(t_{irr})$ as a function of isotope half-life.

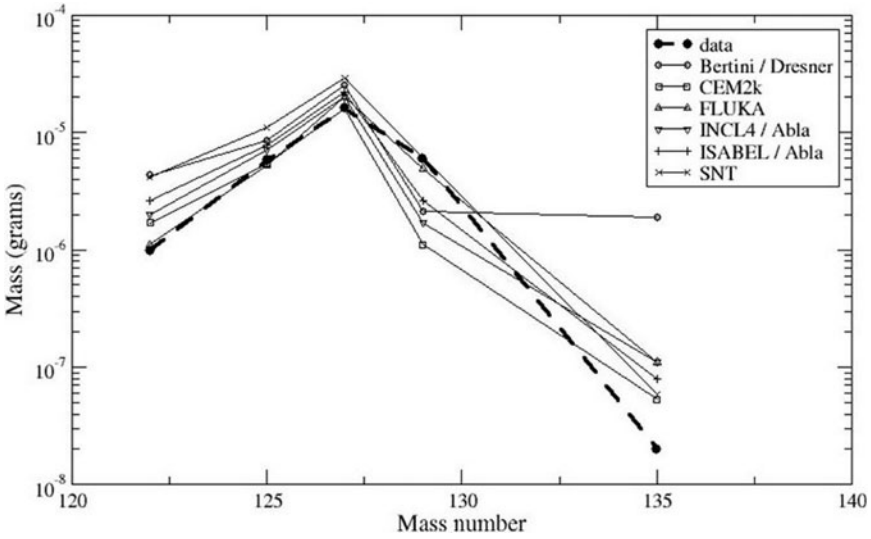

Fig. 7. Measured and calculated xenon mass in the expansion volume after 2 days of irradiation and 15 h of cooling calculated with the sampling factor deduced from scenario s1.

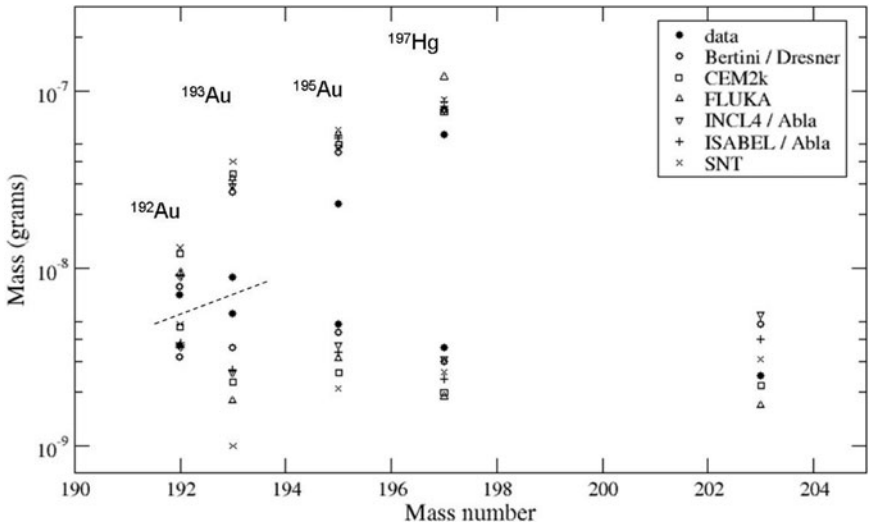

Fig. 8. Lower limit of measured and calculated gold and mercury masses in the expansion volume after 2 days of irradiation and 15 h of cooling.

$$P_d(\Delta t) = \exp(-\lambda \cdot \Delta t) \ . \tag{8}$$

Let us consider that the irradiation begins at $t = 0$. We call t_r the time at which the released stop and t_m the time at which the activity measurement is made, with the relation $0 \leq t_r \leq t_m$. The released isotope amount $N_r(t_r, t_m)$ at time t_m is then given by

$$N_r(t_r, t_m) \approx \int_0^{t_r} g(t) \cdot \left(\frac{t_r - t}{\tau} \right) \cdot dt \tag{9}$$

if $g(t)$ obeys the following relation: $g(t) = N_c(t) \cdot \exp(-\lambda \cdot (t_m - t))$.

$N_c(t)$ represents the nuclide production rate given by the temporal derivative of the absolute created amount $N_a(t)$, excluding the decay contribution. $N_a(t)$ is not directly accessible by the evolution calculation. As a consequence, the concerned nuclides are set as stable in the file that contains radioactive nuclide parameters used by the evolution code CINDER'90. The result of the calculation provides directly $N_a(t)$, which leads to $N_c(t)$ after a derivation in time.

Also, the total amount $N_t(t_m)$ of nuclides generated before the time t_r and present at t_m inside and outside the LBE taking decay into account is given by

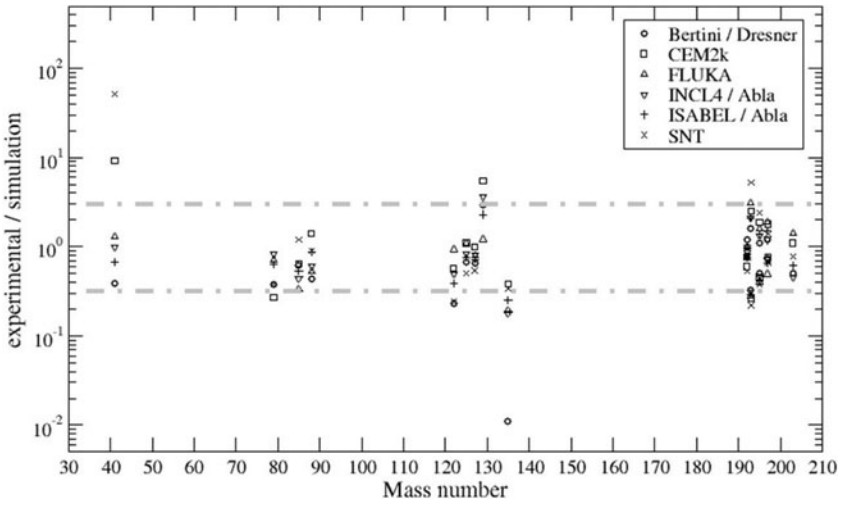

Fig. 9. Ratio between experimental and simulated data. The gray dashed-dotted lines show a factor of 3 deviation from experimental data.

$$N_t(t_r, t_m) = \int_0^{t_r} g(t) \cdot dt \ . \tag{10}$$

At a specified temperature, the release fraction $R(t_r, t_m)$ defined as the amount of released atoms per produced atom in the LBE at the measurement time t_m is then given by the following ratio:

$$R(t_r, t_m) = \frac{N_r(t_r, t_m)}{N_t(t_r, t_m)} \ . \tag{11}$$

This leads to the following expression for the factor τ:

$$\tau \approx \frac{1}{R(t_r, t_m)} \left(t_r - \frac{\int_0^{t_r} t \cdot g(t) \cdot dt}{\int_0^{t_r} g(t) \cdot dt} \right) \ . \tag{12}$$

The LBE temperature has been measured during irradiation and the range near the LBE free surface was between 290°C during irradiation and 220°C during standby.[23] Since the release dependency with the temperature is not known, the volatile behavior can be framed by the following hypotheses:

H1: Volatile release is not affected by temperature fluctuations, which implies that the release is constant during the irradiation and the 15 h of cooling according to the irradiation profile showed in Fig. 4. That implies that $t_r = t_m$.

H2: The volatile nuclide release at 220°C is negligible compared to the release at 290°C, and t_r is then the time the irradiation stopped, 15 h before the activities measurement at t_m.

We consider for the calculation of τ that $R(t_r, t_m)$ is given by the estimated value of the ratio $R(t_{irr})$ with the associated uncertainty. Estimation of τ has been done from the average value obtained with INCL4/ABLA and the error comes from the uncertainty on $R(t_{irr})$, which is dominant. The calculation for noble gases provides for the hypotheses H1 and H2, respectively:

$$\tau_{NG\text{-}H1} = (31 \pm 20) \text{ days} \tag{13}$$

and

$$\tau_{NG\text{-}H2} = (4.7 \pm 3.1) \text{ days} \ . \tag{14}$$

It is worth noting that there is a high deviation on the parameter τ according to the considered hypothesis. A dedicated experiment aiming at defining the temperature dependency of the release rate of noble gases could be a possible way to deduce from the present data a more precise value for this parameter.

V. HYDROGEN AND HELIUM PRODUCTION

During the 6-month irradiation, the pressure in the expansion volume was measured by means of two pressure transducers (see Fig. 2). A pressure evolution model based on calculations has been realized following these assumptions:

1. Perfect gas behavior is assumed.
2. Pressure buildup comes from hydrogen and helium isotopes, with only a negligible fraction coming from other noble gases and from mercury.
3. Hydrogen combines instantaneously into H_2.
4. Initial pressure is a free parameter.

5. The hydrogen and helium release time is lower than the characteristic time of the irradiation.

The pressure evolution is then given by

$$P(t) = \frac{1}{V(t)}\left(V(0)P_0 + \frac{RT(t)n(t)}{N_a}\right) , \qquad (15)$$

where $V(t)$ is the expansion volume. The pressure depends on LBE volume evolution, which is a function of its temperature $T(t)$, which increases when the beam is on target. N_a is the Avogadro constant and $n(t)$ is the amount of gas atoms, expressed as the sum of hydrogen, deuterium, tritium, and helium:

$$n(t) = \frac{n_{\mathrm{H}}(t) + n_{\mathrm{D}}(t) + n_{\mathrm{T}}(t)}{2} + n_{\mathrm{He}}(t) \ . \qquad (16)$$

The temperature evolution $T(t)$ is measured by an in-line thermocouple. By fitting the initial pressure P_0, the pressure evolution was calculated. In Fig. 10 the results are compared to the measured pressures. Measured and calculated pressures are in fair agreement. The shape of the experimental pressure is not reproducible without a nonlinear gas leakage term, which is not conceivable. The integrated amounts of released hydrogen and helium agree with experiment better than 25%. We present as a consequence simulated production of hydrogen and helium normalized for a proton source in Table IV. The results obtained with the INCL4/ABLA version used in the MCNPX version used are known to not be relevant for D, T, and ^{3}He (Ref. 24), so they were not included. Future versions of INCL4/ABLA will include those light particle emissions.[25]

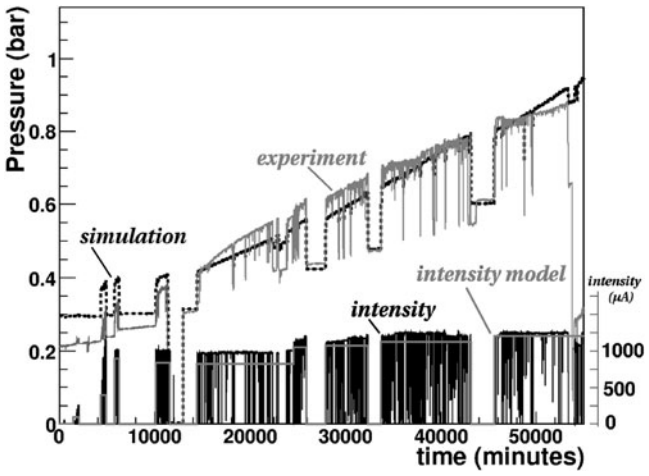

Fig. 10. Experimental (gray line) and calculated (black dots) pressure evolution superposed with experimental (green line) and average (blue line) proton beam intensity (color online).

TABLE IV

Calculated Production Rate per Source Proton of Hydrogen and Helium Isotopes in the Target

	Bertini/Dresner	INCL4/ABLA	ISABEL/ABLA
^{1}H	1.8	1.6	1.43
^{2}H	8.9×10^{-2}	—	—
^{3}H	4.8×10^{-2}	—	—
^{3}He	1.3×10^{-3}	—	—
^{4}He	0.20	0.17	0.30
	CEM2k	FLUKA 2008	SNT
^{1}H	1.3	1.16	1.27
^{2}H	0.4	0.14	0.21
^{3}H	0.1	0.13	5.7×10^{-2}
^{3}He	3.1×10^{-2}	5.3×10^{-3}	0.13
^{4}He	0.19	0.40	

VI. CONCLUSIONS

The MEGAPIE experiment has provided relevant information on spallation target neutronic and nuclear issues. The gas and volatile production is a major point concerning ADS safety. We have presented in this paper a method to estimate the released quantity of noble gases and mercury. If noble gases are expected to be totally released, only about 10^{-2} has been liberated by the LBE after 2 days of operation. The fact that our calculations give comparable results for Ar, Kr, and Xe underlines a similar release mechanism for noble gases. We mention that an additional measurement performed 2 months after the beginning of the experiment showed that the release was almost total. This is in agreement with the estimated parameter representing the release velocity. Mercury and gold have been measured and the lower limit of the expected release fraction has been extracted by considering three scenarios related to mercury diffusion in the CGS. In addition, the necessity to improve metastable state nuclide production in Monte Carlo calculations is emphasized in this work. Finally, hydrogen and helium release have been observed via the pressure buildup in the expansion volume. The pressure evolution has been well reproduced by simulation codes.

ACKNOWLEDGMENT

We would like to express our gratitude to E. N. Messomo for his fine rereading.

REFERENCES

1. EUROPEAN TECHNICAL WORKING GROUP ON ADS, *A European Roadmap for Developing ADS for Nuclear Waste Incineration*, ENEA (Apr. 2001).

2. G. S. BAUER, M. SALVATORES, and G. HEUSENER, "MEGAPIE, a 1 MW Pilot Experiment for a Liquid Metal Spallation Target," *J. Nucl. Mater.*, **296**, 17 (2001).

3. L. ZANINI, J. C. DAVID, A. Yu. KONOBEYEV, S. PANEBIANCO, and N. THIOLLIÈRE, "Neutronic and Nuclear Post-Test Analysis of MEGAPIE," PSI 08-04 (2008).

4. *Accelerator-Driven Systems (ADS) and Fast Reactors (FR) in Advanced Nuclear Fuel Cycles: A Comparative Study*, p. 152, Nuclear Energy Agency, Organisation for Economic Cooperation and Development (2002).

5. J. NEUHAUSEN, "Gas Phase Concentrations of Volatile Nuclear Reaction Production in the MEGAPIE Expansion Tank," PSI MPR-3-NJ18-002/0 (2005).

6. A. FASSO, A. FERRARI, J. RANFT, and P. R. SALA, "FLUKA: A Multi-Particle Transport Code," CERN-2005-10, INFN/TC_05/11, SLAC-R-773 (2005).

7. D. B. PELOWITZ, "MCNPX User's Manual, Version 2.5.0" (2005).

8. W. B. WILSON, T. R. ENGLAND, and P. MÖLLER, "A Manual for CINDER'90, Version 06.1 Codes and Data," Advanced Fuel Cycle Program (Feb. 20, 2006).

9. Yu. A. KOROVIN, A. Yu. KONOBEYEV, and P. E. PERESLAVTSEV, "The Code for the Calculation of Nuclide Composition and Activity of Irradiated Materials," *J. Yadernye Konstanty (Nucl. Constants)*, **3–4**, 117 (1992).

10. J. C. DAVID et al., "Benchmark Calculations on Residue Production Within the EURISOL DS Project, Part I: Thin Targets," DAPNIA-07-59, CEA Saclay (2006).

11. J. C. DAVID et al., "Benchmark Calculations on Residue Production Within the EURISOL DS Project, Part II: Thick Targets," DAPNIA-07-04, CEA Saclay (2007).

12. H. W. BERTINI, "Intranuclear-Cascade Calculation of the Secondary Nucleon Spectra from Nucleon-Nucleus Interactions in the Energy Range 340 to 2900 MeV and Comparisons with Experiment," *Phys. Rev.*, **188**, 1711 (1969).

13. L. DRESNER, "EVAP: A Fortran Program for Calculating the Evaporation of Various Particles from Excited Compound Nuclei," ORNL-TM-196, Oak Ridge National Laboratory (1962).

14. A. BOUDARD et al., "Intranuclear Cascade Model for a Comprehensive Description of Spallation Reaction Data," *Phys. Rev. C*, **66**, 044615 (2002).

15. A. R. JUNGHANS et al., "Projectile-Fragment Yields as a Probe for the Collective Enhancement in the Nuclear Level Density," *Nucl. Phys. A*, **629**, 635 (1998).

16. Y. YARIV and Z. FRAENKEL, "Intranuclear Cascade Calculation of High-Energy Heavy-Ion Interactions," *Phys. Rev. C*, **20**, 2227 (1979).

17. S. G. MASHNIK and A. J. SIERK, "CEM2k: Recent Developments in CEM," *Proc. 4th Int. Topl. Mtg. Nucl. Applications and Accelerator Technology (AccApp 2000)*, Washington, D.C., pp. 328–341 (2000).

18. S. PANEBIANCO et al., "Neutronic Characterization of the MEGAPIE Target," *Ann. Nucl. Energy*, **36**, 350 (2009).

19. R. E. PRAEL and W. B. WILSON, "Nuclear Structure Libraries for LAHET and MCNPX," *Proc. 4th Workshop on Simulating Accelerator Radiation Environments*, Knoxville, Tennessee, September 13–16, 1998, p. 183, Oak Ridge National Laboratory (1998).

20. R. A. FORREST, J. KOPECKY, and J.-Ch. SUBLET, "The European Activation File: EAF-2007 Neutron-Induced Cross Section Library," EASY Documentation Series UKAEA FUS 535 (2007).

21. A. Yu. KONOBEYEV, C. H. M. BROEDERS, U. FISCHER, L. MERCATALI, I. SCHMUCK, and S.P. SIMAKOV, "The Proton Activation Data File PADF-2007 in ENDF-6 Format," Int. Conf. Nuclear Data for Science and Technology, 2007.

22. H. L. RAVN, "Experiments with Intense Secondary Beams of Radioactive Ions," *Phys. Rep.*, **54**, 201 (1979).

23. S. DEMENTJEVS, Personal Communication (2010).

24. S. LERAY et al., "Recent Improvements of Spallation Models for Better Predictions of Helium and Tritium Production," DAPNIA-07-286 (2008).

25. J. C. DAVID, "INCL4.5 and Abla07: Improved Versions of the Intranuclear Cascade (INCL4) and Deexcitation (Abla) Models," SATIF10 (2010).